Theor Chem Acc (1998) 100:171–182
DOI 10.1007/s002149800m49

Theoretical
Chemistry Accounts

Regular article

Excited states of acetylene: a CASPT2 study*

Karsten Malsch, Rupert Rebentisch, Petra Swiderek, Georg Hohlneicher

Institut für Physikalische Chemie, University of Cologne, Luxemburgerstrasse 116, D-50939 Cologne, Germany

Received: 11 June 1998 /Accepted: 30 July 1998 / Published online: 19 October 1998

Abstract. Valence and low-lying Rydberg states of acetylene (C_2H_2) are reexamined in the singlet as well as in the triplet manifold. The major goal of this work is a better understanding of the valence states that contribute to the low-energy electron-energy-loss spectrum recorded under conditions where transitions to triplet states are enhanced. An appropriate theoretical treatment of these states has to include the low-lying Rydberg states because of their energetic proximity to some of the valence states. The CASSCF/CASPT2 method provides a suitable framework for such a task. For some important states the geometry was optimized at the CASPT2 level to allow a comparison with the results of other highly accurate methods that have been applied to acetylene in the past.

Key words: Acetylene – Singlet and triplet states – Valence and Rydberg states – CASPT2 calculations – Linear and bent geometries

1 Introduction

The interpretation of the electronic spectra of acetylene (C_2H_2) provides a particularly challenging problem to quantum chemistry. The highest occupied (HOMO) and the lowest unoccupied (LUMO) orbital are both degenerate. A one-electron excitation from HOMO to LUMO leads to several excited singlet and triplet states. Except for possibly $S_4(^1\Sigma_u^+)$, where no reliable information is available, all of these states are known to be instable with respect to the linear geometry adopted by the ground state. The possibility of cisoid and transoid deformations leads to a further increase in the number of accessible excited valence states and to strongly non–vertical excitations. Figure 1 provides a schematic view of this situation. As will be discussed later, it has to be mentioned that the situation displayed in Fig. 1 is oversimplified for some of the singlet and triplet states higher in energy (S_2, S_3, T_3, and T_4). Here, only less symmetric structures seem to represent stable geometries. Also, curve crossings can appear in more asymmetric structures.

An additional complication is caused by the fact that, owing to the smallness of the system, the lowest Rydberg states are energetically not well separated from the valence states. The electron energy loss (EEL) spectra [1] shown in Fig. 2 give a rough overview of the available experimental information. The onset of transitions with pronounced Rydberg character is clearly obvious around 8 eV [2, 3], but there is still some ongoing discussion about the valence character of some of the signals in the region between 8 eV and the first ionization potential located at 11.41 eV [4]. Among the valence states the most detailed information is available for the *trans* bent 1^1A_u state whose vibronic levels have been detected from the adiabatic transition at 5.23 eV up to 6.75 eV [5, 6]. The assignment of other singlet states is less certain. A band appearing at 6.71 eV in the UV spectrum was assigned to 1^1B_u [7] and a band around 7.2 eV in the singlet-dominated EEL spectrum (Fig. 2, upper panel) to $1^1\Delta_u$ [1]. Nothing is known about the singlet states 1^1A_2 and 1^1B_2 expected to lie below $1^1\Delta_u$. With regard to the triplet manifold, recent high-resolution EEL investigations revealed that the band between 4.4 eV and 5.6 eV which was assigned to $1^3\Sigma_u^+$ by Allan [1] results most likely from a superposition of at least two different triplet transitions [8]. A complicated band observed under the same conditions between 5.6 eV and 7.0 eV is also ascribed to singlet and triplet transitions [1, 8].

Because of the complicated electronic and geometric structure of some of its electronically excited states, acetylene has been the subject of a large number of theoretical investigations [9–24]. The first comprehensive examination of valence and Rydberg states of linear and bent singlet and triplet acetylene dates back to Demoulin [23] and Demoulin and Jungen [22]. The importance of bent geometries had been already stressed by Kammer

*Dedicated to Prof. Dr. Wilfried Meyer on the occasion of his 60th birthday

Correspondence to: G. Hohlneicher
e-mail: gehohln@fock.pc.uni-koeln

[24] in 1970. Although the calculations of Demoulin are methodically simple by today's standards, they are still the only source that provides theoretical information on triplet Rydberg states. The first geometry optimizations for the two lowest triplet states of *cis* and *trans* bent acetylene came from Wetmore and Schaefer [21]. An improved picture of valence and Rydberg states in the singlet manifold was given by Peric et al. [17, 19, 20] in a series of papers between 1984 and 1987. Using the MRD-CI method, these authors calculated one-dimensional cross sections through the potential energy surface (PES) of several excited states for the bending, CC stretch, and CH stretch degrees of freedom. The influence of the Renner-Teller effect was also examined in this study. At the same time, Lischka and Karpfen [18] performed an extensive study of the valence states of acetylene using CI and MCSCF approaches. They reported geometries, excitation energies, and harmonic vibrational frequencies for the first three singlet and the lowest four triplet excited states. Yamaguchi et al. [14] recently repeated this kind of investigation for the four lowest triplet states at an elaborate level of theory, applying methods up to CCSD(T) and QZ (3*df*,3*pd*) basis sets.

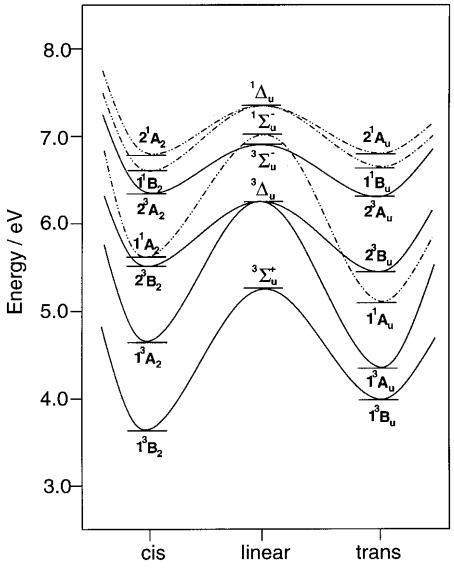

Fig. 1. Schematic overview of the (π,π^*) excited valence states of acetylene. The triplet states are shown as *solid lines*. The *curves* symbolize a possible relaxed pathway from the linear geometries to the minima in C_{2h} and C_{2v} symmetry. The energies correspond to the calculated CASPT2 results. The S_4 state ($^1\Sigma_u^+$) is not shown in the figure

The interpretation of the observed spectral patterns is further complicated by the possible appearance of excited states that result from double excitations. These excitations should lead to bent structures with excitation energies below the first ionization threshold. An example is the *trans* bent $\tilde{C}'$ state observed by Lundberg et al. [25] at 7.72 eV and theoretically described by Lievin [16]. Most recently, two facts kept the interest in theoretical investigations of acetylene alive. The first was the introduction of algorithms for searching and characterizing transition states and reaction paths on the PES. These methods were used for the description of the vinylidene-acetylene rearrangement [13, 15] or the S_1 photodissociation [9, 10]. The second source was the experimental observation of a triplet perturber of the first excited singlet state by Zeeman anticrossing spectroscopy [26, 27]. This observation led to several new experimental [28, 29] and theoretical [9–12] investigations of stationary points on the PES of the low-lying singlet and triplet states.

In spite of this large number of theoretical investigations, the interpretation of the UV [3] and EEL [1, 8, 30–32] spectra of acetylene still poses open questions. The only well-assigned state is the *trans* bent S_1 state (1^1A_u) [5, 6]. The obvious assignment problems result from possible Rydberg/valence mixing [3, 33], Renner-Teller splitting [19, 34], and the low intensity of some 0,0

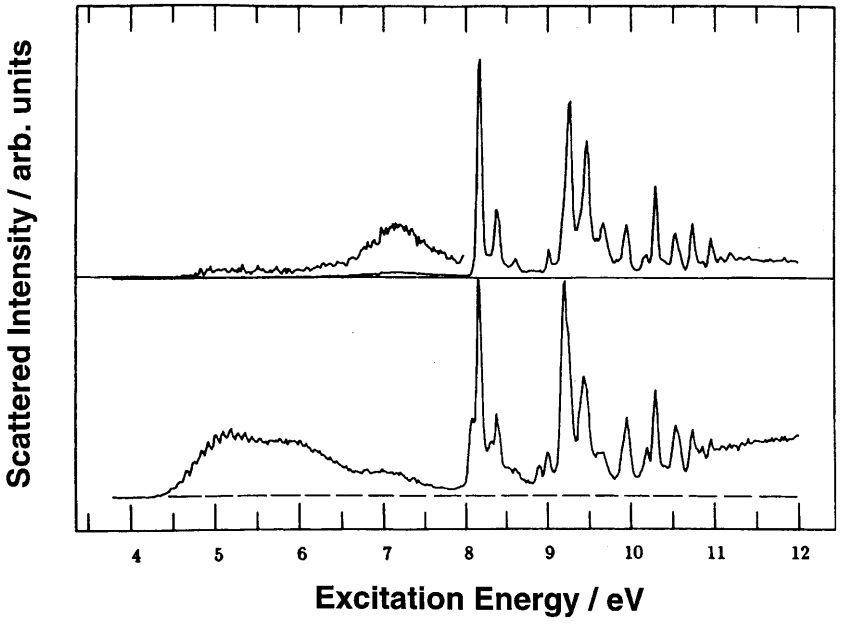

Fig. 2. Gas-phase electron-energy-loss spectrum of acetylene (from [1]) recorded at high (*upper panel*) and low residual energy. The high residual energy spectrum is dominated by optically allowed transitions. The low-energy spectrum allows the detection of optically forbidden transitions (e.g. detection of triplet states)

transitions combined with long vibronic progressions that result from the change in the molecular structure with $\pi\pi^*$ excitation [5, 6]. The major goal of the present work is to reinvestigate the valence and the first Rydberg states of acetylene with equal accuracy and to compare the results obtained with the findings from recently measured high-resolution EEL spectra [8] and with other experimentally available information on the low-lying singlet and triplet states.

2 Methods and computational details

2.1 Symmetry considerations

Acetylene (C_2H_2) is linear in its electronic ground state (point group $D_{\infty h}$). Therefore the description of the $1^1\Sigma_g^+$ electronic ground state by means of molecular orbital (MO) theory is straightforward. The *s* orbitals of carbon and hydrogen together with the carbon p_z orbitals can be used to construct σ orbitals with the classification σ_g and σ_u. The remaining four carbon p_x and p_y orbitals lead to a degenerate pair of bonding and a degenerate pair of antibonding π orbitals characterized as π_u and π_g in point group $D_{\infty h}$. The configuration of the ground state is $(1\sigma_g)^2\ (1\sigma_u)^2\ (2\sigma_g)^2\ (2\sigma_u)^2\ (3\sigma_g)^2\ (1\pi_u)^4\ (1\pi_g)^0\ (3\sigma_u)^0$. The low-lying excited valence states are expected to result from the $\pi\pi^*$ excitation. The configuration $....(1\pi_u)^3\ (1\pi_g)^1$ yields the following electronic states: $^{1,3}\Sigma_u^+$, $^{1,3}\Sigma_u^-$, and $^{1,3}\Delta_u$. Figure 1 shows the approximate sequence of these states.

The states that result from the $\pi\pi^*$ excitation are unstable with respect to distortion along the CCH bending angle. The reduction of the bond order from three to two leads to energetically favored *cis* and *trans* bent structures for these excited states. The Renner-Teller distortion of the degenerate Δ state is also expected to act in favor of a bent structure for the lower of the two resulting states. As long as the four atoms stay in one plane, the *trans* bent structure belongs to point group C_{2h} and the *cis* bent structure to C_{2v}. If, as several high-quality calculations indicate [9,10], some states deviate from these symmetries, the symmetry becomes C_S as long as the four atoms remain in plane. Deviation from planarity reduces the symmetry to C_2 or even C_1. The correlation between the irreducible representations (IRREP) of the point groups $D_{\infty h}$, D_{2h}, C_{2h}, and C_{2v} is shown in Table 1.

Table 1. Correlation of irreducible representations (IRREP) between the different relevant point groups (C_{2h}: $z \rightarrow x, y$; C_{2v}: $z \rightarrow y$, see [2]). The last column indicates to which IRREP excitations from the highest occupied orbital (π) to the indicated orbital belong

$D_{\infty h}$	D_{2h}	C_{2h}	C_{2v}	Upper orbital
Σ_g^+	A_g	A_g	A_1	p_π
Σ_g^-	B_{1g}	B_g	B_1	p_π
Σ_u^+	B_{1u}	B_u	B_2	$\pi^*(T_1, S_4)$, d_π
Σ_u^-	A_u	A_u	A_2	π^* (S_1, T_4), d_π
Π_g	$B_{2g} + B_{3g}$	$A_g + B_g$	$A_2 + B_2$	p_σ
Π_u	$B_{2u} + B_{3u}$	$A_u + B_u$	$A_1 + B_1$	s, d_σ, d_δ
Δ_g	$A_g + B_{1g}$	$A_g + B_g$	$A_1 + B_1$	p_π
Δ_u	$A_u + B_{1u}$	$A_u + B_u$	$A_2 + B_2$	π^* $(S_{2,3}, T_{2,3})$, d_π
Φ_g	$B_{2g} + B_{3g}$	$A_g + B_g$	$A_2 + B_2$	
Φ_u	$B_{2u} + B_{3u}$	$A_u + B_u$	$A_1 + B_1$	d_δ

Electronic structure calculations on molecules that belong to non-Abelian point groups are prone to special problems. None of the widely used quantum chemical program packages is able to perform the calculation with the full symmetry information. Instead, the calculation is done within the smallest Abelian subgroup. In the case of acetylene we had to calculate the electronic ground state and the vertically excited states using D_{2h} symmetry. Consequently the degeneracy of Π, Δ, and Φ states is no longer assured by symmetry constraints. Orbitals which do not mix under full symmetry are no longer prevented from doing so in the course of an iterative calculation. In all calculations presented in this paper, special care was taken to omit this problem. The energies of the π orbitals were averaged after each cycle and all calculations that showed more than a very small amount of the above-mentioned mixing were rejected.

2.2 Methods of calculation

The CASSCF/CASPT2 method was used to account for electron correlation effects [35–38]. The applied basis sets were the following general contracted ANO [39] sets [40]: 14*s*-, 9*p*-, 4*d*-, and 3*f*-type

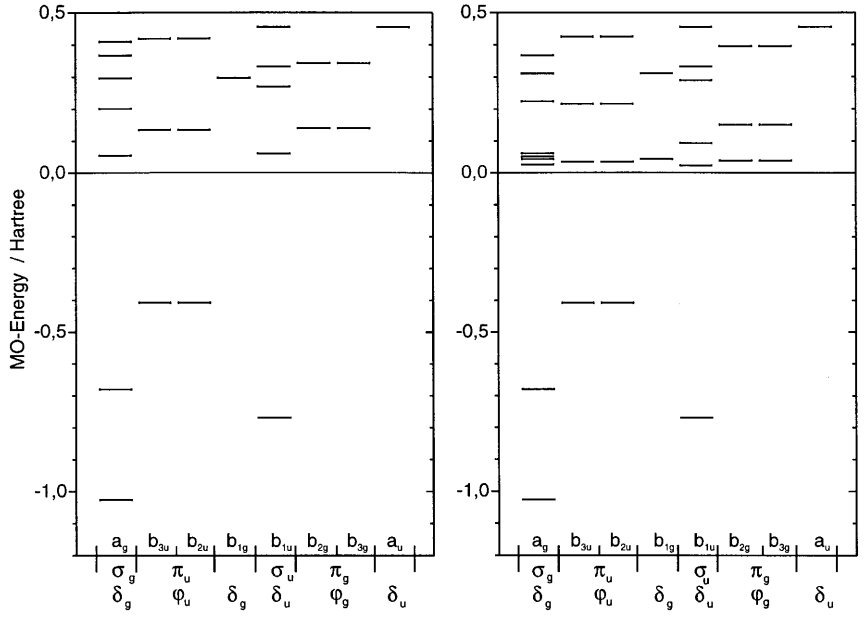

Fig. 3. *Left panel*: SCF-MOs obtained with the valence basis (see text for definition). *Right panel*: SCF-MOs obtained with the augmented basis (see text for definition). The orbitals are labeled with respect to $D_{\infty h}$ and D_{2h}, the symmetry used for the calculations. Not included are, in both cases, the orbitals $1\sigma_g$ and $1\sigma_u$ at about -11.2 Hartree

primitive gaussians contracted to a 4*s*, 3*p*, 2*d*, and 1*f* set for carbon and 8*s*-, 4*p*-, and 3*d*-type primitive gaussians contracted to a 3*s*, 2*p*, and 1*d* set for hydrogen. The total of 88 basis functions that results from these atomic basis sets is refered to as *valence basis* in the rest of the text. To treat the Rydberg transitions and to improve the description of the valence states in cases where Rydberg transitions come into play, the valence basis was augmented by a special Rydberg basis set [36]. Eight *s*-, eight *p*-, and eight *d*-type primitive gaussians, all localized at the center of the molecule, were added to the valence basis. These orbitals where contracted to a 1*s*, 1*p*, and 1*d* set. The contraction coefficients were obtained from a CASSCF calculation of the $^2\Pi_u$ ground state of $C_2H_2^+$. The general contraction matrix was determined from the lowest virtual molecular orbitals of the cation that were not found inside the active space after the calculation. The basis that consists of the valence basis and the contracted Rydberg basis is called *augmented basis* hereafter. Figure 3 shows the SCF orbital energies obtained with the valence basis (left panel) and the augmented basis (right panel), respectively. The nine lowest virtual orbitals on the right side are the Rydberg orbitals. As we do not consider transitions to higher Rydberg shells, we do not need to include more than one set of contracted Rydberg orbitals in our calculations.

To specify the active spaces (AS) from which we started the CASSCF calculations, we first discuss the linear molecule. The *full valence space* defined in Table 2 includes 10 electrons and 10 orbitals corresponding to the 10 valence atomic orbitals of acetylene. The only two occupied orbitals not included in the full valence space ($1\sigma_g$ and $1\sigma_u$) are combinations of the carbon 1*s* orbitals which lie about 10 Hartree below the first orbital included in the AS. Test calculations with AS of different size showed that the results for the ground state and the excited valence states could be improved by inclusion of the orbitals $2\pi_g$ and $2\pi_u$. The resulting active space is called *extended valence space* (see Table 2). This AS was used for all calculations that were done with the valence basis.

Inclusion of the nine Rydberg orbitals that result from the augmented basis set into the full valence space would lead to an AS with 10 electrons and 19 orbitals. An AS of this size cannot be handled by any of the available programs. Therefore we used two different ASs for calculations that included Rydberg states. An interference between valence and Rydberg states is only possible for the symmetries Σ_u^+, Δ_u, and Σ_u^-. As long as we consider only excitations that depart from the occupied π orbitals ($1\pi_u$), the relevant Rydberg orbitals are the π_g (d_π) orbitals. As excitations to the Rydberg π_u (p_π) orbitals which lead to Σ_g^+, Δ_g, and Σ_g^- states are also $\pi\pi^*$–type excitations, these orbitals were included in what is called π *space* in Table 2. For all further Rydberg states (Π_g, Π_u, Φ_u) we used the AS specified as σ, δ *space* in Table 2. In addition to the occupied valence orbitals, this space includes five Rydberg orbitals [$s(a_g)$, $p_\sigma(b_{1u})$, $d_\sigma(a_g)$, $d_\delta(a_g, b_{1u})$] and, to assure consistency with the other AS, the $2\pi_g$ orbitals. These two AS were used for all calculations that were done with the augmented basis.

To avoid the intruder state problem a level-shift technique was applied in connection with the CASPT2 calculation (LS-CASPT2 [41–44]) in all cases where the augmented basis was used. Table 3 shows the influence of the level shift on some vertical excitation energies and on the weight of the CASSCF reference wavefunction. At a level shift of 0.3 au the excitation energies become fairly stable and the weights uniform with one exception: $2^1\Sigma_u^+$, the highest valence excited state in the singlet manifold. As a level shift of 0.3 au has already been found to be adequate in other applications [44], we used this value in all further calculations. Since $2^1\Sigma_u^+$ is not described satisfactorily with the π space, a different AS, called $2^1\Sigma_u^+$ *space* in Table 2, was used for this state.

Table 2. Different active spaces mentioned in the text

Active space	Orbitals
Full valence	$2\sigma_g$, $3\sigma_g$, $2\sigma_u$, $1\pi_u$, $1\pi_g$, $4\sigma_g$, $3\sigma_u$, $4\sigma_u$
Extended valence	full valence plus $2\pi_u$ and $2\pi_g$
π space	full valence plus $2\pi_u$ (p_π) and $2\pi_g$ (d_π)
σ,δ space	$2\sigma_g$, $3\sigma_g$, $2\sigma_u$, $1\pi_u$, $1\pi_g$, $2\pi_g$, $\sigma_g(s)$, σ_g ($d\sigma$), $\sigma_u(p_\sigma)$, Δ_g ($d\delta$)
$2^1\Sigma_u^+$ space	full valence plus $2\pi_g$ and $3\pi_g$

For the bent structures of acetylene we used the valence basis and an AS which corresponds to the extended valence space of the linear molecule. For these structures the relevant valence states lie well below the onset of the first Rydberg series, so that we do not need to bother with a possible interference of valence and Rydberg states.

Geometries were optimized at the CASSCF level. For several low-lying states these optimizations were supplemented by optimizations at the CASPT2 level with single point calculations on a two-dimensional (CH and CC bond length) or three-dimensional (bond lengths and CCH bond angle) grid. For the latter calculations we used a *reduced valence space* which consisted of only nine active orbitals and eight active electrons, i.e. in comparison to the *full valence space* the second totally symmetric MO ($2a_g/2a_1$) was kept inactive. The distance between the grid points at the end of the optimization was 0.001 Å for the bond lengths and 1° for the bond angle.

All calculations were performed with the *MOLCAS* suite of programs [45].

3 Results and discussion

3.1 Ground state geometry

The *valence basis set* and the AS called the *extended valence space* (see Sect. 2.2) were used for the treatment of the linear ground state. The bond lengths of the CASSCF optimized structure are $r_{CC} = 1.216$ Å and $r_{CH} = 1.073$ Å. At the CASPT2 level we find $r_{CC} = 1.217$ Å and $r_{CH} = 1.066$ Å. The latter are the bond lengths used for the ground state in all further calculations. The ground state geometry is only slightly influenced by the PT2 correction. Almost all of the correlation important for the description of the ground state is already included at the CASSCF level. This is in accord with the 96.9% weight of the CASSCF wavefunction in the CASPT2 wavefunction of the ground state.

The CASPT2 result is in good agreement with the experimental bond lengths of $r_{CC} = 1.2026$ Å and $r_{CH} = 1.0622$ Å [46]. Among other studies that applied highly correlated methods to acetylene, only the CCSD(T) calculation with TZ2P basis of Stanton et al. [13] ($r_{CC} = 1.2017$ Å and $r_{CH} = 1.0616$ Å) is closer to the experimental values. CCSD(T) and other methods like CCSD, CISDT, and CISD (see [11]) yield larger deviations from the experimental values when used in connection with smaller basis sets (DZP). In all these calculations the bond lengths are fairly overestimated. This is believed to be a general tendency in correlated calculations which are not well balanced because of a too small basis set. We are sure that a further increase in the size of the basis set would lead to an even better agreement between experiment and theory, but such an investigation is beyond the scope of the present study.

3.2 Vertical excitations

Vertical excitations were calculated with the augmented basis set and, depending on the symmetry of the final state, with the π or with the σ, δ space. The results are shown in Table 4 for the singlet states and in Table 5 for

Table 3. Influence of the *CASPT2 level shift* (*LS*) on the calculated CASPT2 excitation energies (ΔE) and the weight of CASSCF reference wavefunctions (Ref/). All calculations were performed using the *augmented basis* and the *π space* as active space

LS-CASPT2											
State	D_{2h}	LS = 0.0 Hartree		LS = 0.1 Hartree		LS = 0.2 Hartree		LS = 0.3 Hartree		LS = 0.4 Hartree	
		ΔE (eV)	Ref. (%)	ΔE (eV)	Ref. (%)	ΔE (eV)	Ref. (%)	ΔE (eV)	Ref. (%)	ΔE (eV)	Ref. (%)
$1^1\Sigma_g^+$	^1A_g	−77.1683045860	96.2	−77.1681695334	96.5	−77.1678091454	96.7	−77.1672762050	96.9	−77.1666098023	97.1
$1^1\Sigma_u^-$	^1A_u	6.87	85.0	6.95	91.7	7.02	93.4	7.07	94.3	7.11	94.9
$1^1\Delta_u$	$^1B_{1u}$	7.31	90.9	7.34	93.2	7.37	94.1	7.40	94.7	7.43	95.2
$1^1\Delta_u$	^1A_u	7.25	84.1	7.34	91.4	7.42	93.4	7.48	94.4	7.53	95.0
$2^1\Sigma_u^+$	$^1B_{1u}$	27.61	2.7	0.22	29.1	6.97	65.1	8.74	79.2	9.58	85.4
$1^1\Sigma_u^+$	$^1B_{1u}$	9.55	90.7	9.59	94.4	9.62	95.3	9.65	95.9	9.67	96.2
$2^1\Delta_u$	^1A_u	9.60	87.7	9.66	93.8	9.70	95.0	9.73	95.7	9.76	96.1
$2^1\Sigma_u^-$	^1A_u	9.73	90.5	9.76	94.6	9.79	95.5	9.81	96.0	9.83	96.3
$2^1\Delta_u$	$^1B_{1u}$	9.84	93.3	9.86	94.9	9.87	95.5	9.88	95.9	9.90	96.3
$1^3\Sigma_u^+$	$^3B_{1u}$	−53.32	0.2	4.94	87.9	5.17	93.4	5.26	94.8	5.31	95.5
$1^3\Delta_u$	$^3B_{1u}$	5.36	49.0	5.91	87.7	6.11	92.4	6.22	94.0	6.29	94.9
$1^3\Delta_u$	^3A_u	5.82	70.3	6.04	90.5	6.16	93.3	6.22	94.4	6.28	95.1
$1^3\Sigma_u^-$	^3A_u	6.51	69.3	6.76	89.6	6.90	92.9	6.99	94.3	7.05	95.0
$2^3\Delta_u$	$^3B_{1u}$	9.74	88.9	9.79	95.1	9.81	95.9	9.83	96.4	9.84	96.7
$2^3\Delta_u$	^3A_u	9.82	93.0	9.84	95.5	9.85	96.1	9.83	96.4	9.87	96.7
$2^3\Sigma_u^+$	$^3B_{1u}$	9.82	94.6	9.83	96.0	9.84	96.3	9.84	96.6	9.85	96.8
$2^3\Sigma_u^-$	^3A_u	9.73	88.0	9.79	94.6	9.82	95.6	9.84	96.1	9.86	96.5

the triplet states. The states are labeled with respect to $D_{\infty h}$, the point group of the linear molecule, and also with respect to D_{2h}, the symmetry in which the calculations were actually done. As all important one-electron excitations start from the occupied π orbitals it is sufficient to specify the upper orbital of the dominating configurations to define the character (Char.) of the excited state. The upper part of the tables shows the results of state averaged calculations. The averaging included four states for the IRREPS A_u, B_{1u}, and B_{2u}/B_{3u} and two states for the IRREPS A_g and B_{1g}. The lower part of the table shows results for a few single-root calculations. All energies are relative to the ground state energy obtained with the appropriate active space. From the CASSCF results we list the excitation energy, the charge at the Rydberg center, the expectation value $\langle r^2 \rangle$ as a measure of the wavefunctions spatial extent and, for the dipole-allowed transitions, the transition dipole moment (TDM) obtained with the RASSI method [47, 48]. For the LS-CASPT2 calculations we show the excitation energy and the weight of the CASSCF reference wavefunction. For comparison we also list results from some other calculations and assignments that were given in various experimental studies.

With a level shift of 0.3 au the weight of the reference wavefunction in the CASPT2 results is between 94% and 97% with one exception: $2^1\Sigma_u^+(\pi\pi^*)$. This state had a weight of only 79% in the state averaged calculation (see Table 3), indicating that the active space we used for this calculation in IRREP B_{1u} is not sufficient to decribe this state. Changing the active space as described in Sect. 2.2 leads to a weight of the reference wavefunction of 95% and to an increase of the excitation energy by about 2 eV. This is a reasonable result as poor reference wavefunctions usually lead to overestimated PT2 corrections. In cases where we are able to compare state-averaged and single-root CASPT2 calculations, the difference is less than 0.2 eV in excitation energy and 2% in the weight of the reference function. The fact that the corresponding CASSCF energies differ by about 1 eV shows that the PT2 correction is able to compensate for most of the deficiencies of a less accurate reference wavefunction. One of the deficiencies of the CASSCF wavefunctions from state-averaged calculations is indicated by the charge at the Rydberg center and by the $\langle r^2 \rangle$ value, which are both considerably reduced in the single-root calculations of the valence states $1^1\Sigma_u^-$, $1^3\Sigma_u^+$, $1^1\Delta_u$, $1^3\Delta_u$, and $1^3\Sigma_u^-$. The comparatively high values in the averaged calculations indicate a stronger Rydberg-valence mixing on the MO level which is significantly reduced in the single-root calculations. Two conclusions can be drawn from this result:

1. The PT2 correction seperates the above-mentioned valence states even further from the Rydberg states with the consequence that Rydberg-valence mixing becomes negligible for these valence states.
2. The PT2 correction is able to correct the energy even for the averaged states that show some mixing on the MO level. Therefore PT2 results seem to be reliable even in cases where some extent of mixing in the MOs cannot be circumvented.

Table 4. Vertical excitation energies of excited Rydberg and valence singlet states

State	Char.	D_{2h}	CASSCF				LS-CASPT2		Literature	
			ΔE (eV)	Charge	$\langle r^2 \rangle$	TDM	ΔE (eV)	Ref. (%)	Exp.	Calc.
$1^1\Sigma_g^+$	G.S.	A_g	–	−0.0101	10.1		–	96.9		
$1^1\Sigma_u^-$	π^*	A_u	8.62	0.1309	14.0		7.07	94.3	7.1[a]	7.42[b],7.21–7.32[f]
$1^1\Delta_u$	π^*	B_{1u}	8.86	0.1256	14.0	–	7.40	94.7	7.2[a]	7.80[b],7.56–7.65[f]
$1^1\Delta_u$	π^*	A_u	8.91	0.2096	17.0		7.48	94.4	7.2[a]	7.80[b],7.56–7.65[f]
$1^1\Pi_u$	s	B_{2u}, B_{3u}	8.60	0.1243	20.8	0.089	8.30	95.6	8.16[a,c,d]	8.42[e],7.92–8.00[f]
$1^1\Pi_g$	p_σ	B_{2g}, B_{3g}	8.67	0.3891	17.5		8.60	96.0	9.01[a,d,g]	8.90[e],8.38–8.46[f]
$1^1\Sigma_g^-$	p_π	B_{1g}	8.96	0.8931	41.3		8.92	96.7		9.29[h],8.92–8.95[f]
$1^1\Delta_g$	p_π	A_g, B_{1g}	9.01	0.8936	41.4		8.96	96.7	9.01[a,d,g], 9.02[i]	9.19[h],8.87–8.90[f]
$2^1\Sigma_g^+$	p_π	A_g	9.19	0.9443	44.1		9.06	96.5	9.21[a,d,g,i]	9.30[e],9.03[f]
$2^1\Pi_u$	d_σ	B_{2u}, B_{3u}	9.76	0.7592	26.3	0.022	9.55	95.7	9.24[c]	9.68[e],9.36–9.44[f]
$1^1\Sigma_u^+$	d_π	B_{1u}	10.14	0.9855	50.5	0.066	9.65	95.9	9.27[c]	9.83[h],9.41–9.58[f]
$2^1\Delta_u$	d_π	A_u	10.36	0.8033	45.2		9.73	95.7	10.00[k]	10.04[h],9.70–9.80[f]
$2^1\Sigma_u^-$	d_π	A_u	10.29	0.8820	48.2		9.81	96.0		10.05[h],9.75–9.80[f]
$2^1\Delta_u$	d_π	B_{1u}	10.48	0.8913	49.1	–	9.88	95.9		10.04[h],9.70–9.80[f]
$1^1\Phi_u$	d_δ	B_{2u}, B_{3u}	10.02	0.9847	71.1	–	9.93	96.0	9.91[c,j]	10.02[e],9.69–9.80[f]
$3^1\Pi_u$	d_δ	B_{2u}, B_{3u}	10.02	0.9841	71.0	0.023	9.93	96.0	9.98[l]	10.03[e],9.69–9.80[f]
$2^1\Sigma_u^+$	π^*	B_{1u}	11.02	0.1474	23.7	0.659	10.65	95.2		9.88[e]
$1^1\Sigma_u^-$	π^*	A_u	7.67	0.0222	11.2		6.96	95.8	7.1[a]	7.42[b]
$1^1\Delta_u$	π^*	A_u, B_{1u}	7.90	0.0332	11.7		7.30	96.0	7.2[a]	7.80[b]
$1^1\Sigma_u^+$	d_π	B_{1u}	9.30	0.8582	43.5	0.137	9.50	97.0	9.27[c]	9.83[h],9.41–9.58[f]

[a] From [1] [b] From [18] [c] From [49]
[d] From [50] [e] From [22] [f] From [20]
[g] From [32] [h] From [23] [i] From [55]
[j] From [60] [k] From [61] [l] From [62]

For the excited singlet valence state $2^1\Sigma_u^+$, Rydberg-valence mixing can no longer be excluded. The calculation predicts a slightly more diffuse wavefunction and an increased charge at the Rydberg center compared to the other valence states. This is not unexpected as $2^1\Sigma_u^+$ is embedded in a manifold of Rydberg states close to the first ionization threshold. The Rydberg states $\Pi_u(s)$, $\Pi_g(p_\sigma)$, and, to some extent, $\Pi_u(d_\sigma)$ are predicted to be somewhat more compact than the other Rydberg states in the singlet as well as in the triplet manifold, but these states do not interfere with the considered valence states.

The degeneracy of $1^1\Delta_u$ is not fully reproduced in the state- averaged calculation, in contrast to the single-root calculation (see Table 4). Correspondingly, a similar deviation is found for the Rydberg state $2^1\Delta_u$. The mixing of orbitals that belong to different symmetries in $D_{\infty h}$ could not be removed completely in our calculation. This may be due to the fact that in the state-averaged calculation the unsatisfactory described $2^1\Sigma_u^+$ state disturbs the other B_{1u} states. The deviations are, however, small (less than 0.1 eV) and need not be regarded as a problem.

The lowest excited singlet state $1^1\Sigma_u^-$ is predicted to lie at 6.96 eV (if available, the single-root results are used for the discussion) followed by the $1^1\Delta_u$ valence state at 7.3 eV. Both values are about 0.5 eV lower than those obtained by Lischka and Karpfen [18]. The experimental estimate for the vertical transition to $1^1\Delta_u$ is 7.2 eV [1]. The first Rydberg series starts with $1^1\Pi_u(s)$ at 8.3 eV, in close agreement with the experimental value of 8.16 eV [1, 49, 50]. Demoulin [22] obtained 8.42 eV and Peric et al. [20] 8.00 eV. The energy gap between the first two singlet valence states and the Rydberg states is about 1 eV for the linear geometry.

The energetically lowest state of triplet multiplicity is $1^3\Sigma_u^+$, located at 5.26 eV, in excellent agreement with the experimental value of 5.2 eV given by Allan [1]. The calculated $S_1 - T_1$ gap is 1.7 eV, i.e. 13 700 cm^{-1}. The degenerate second triplet state ($T_{2,3}$), $1^3\Delta_u$, is predicted at 6.2 eV (again in good agreement with an experimental value of 6.0 eV [1]). The energy gap of almost 1 eV between T_1 and $T_{2,3}$ is somewhat smaller than the gap between S_1 and S_2 (1.3 eV). The calculated fourth triplet state T_4 is $1^3\Sigma_u^-$ at 6.9 eV, only 0.7 eV above $1^3\Delta_u$, and only 0.06 eV below the corresponding singlet state. The near degeneracy of $1^3\Sigma_u^-$ and $1^1\Sigma_u^-$ had already been found in the calculations of Lischka and Karpfen [18]. Allan [1] assigned a band around 7.1 eV in the gas-phase triplet-enhanced EEL spectrum (see Fig. 2, lower panel) to both transitions, but it is not clear whether this band results really from a superposition of these two transitions or only from one of them. Swiderek et al. [8] related a signal at 6.47 eV in the EEL spectrum to $1^3\Sigma_u^-$. We will return to the assignment of this state after the discussion of nonlinear excited valence states.

The first calculated triplet Rydberg state is $1^3\Pi_u(s)$ at 8.19 eV. The calculated triplet-singlet splitting is only 0.11 eV, in close agreement with the experimental value of 0.09 eV. Demoulin [22] found 0.17 eV in his calculation. All three vertically excited triplet states that result from the $\pi\pi^*$ excitation are predicted to lie 1.3 eV or more below the onset of the first Rydberg series. Valence-Rydberg mixing is therefore unlikely and no indication of such mixing is found in the calculations. The energy obtained for $2^1\Sigma_u^+$ from the state-averaged calculation (8.74 eV) is not reliable because of the low weight of the reference wavefunction (see Table 3) and an extremely large PT2 correction of 5.43 eV. The in-

Table 5. Vertical excitation energies of excited Rydberg and valence triplet states.

State	Char.	D_{2h}	CASSCF			LS-CASPT2		Literature	
			ΔE (eV)	Charge	$\langle r^2 \rangle$	ΔE (eV)	Ref. %	Exp.	Calc.
$1^3\Sigma_u^+$	π^*	B_{1u}	6.33	0.0269	10.1	5.26	94.8	5.2[a]	5.61[c]
$1^3\Delta_u$	π^*	B_{1u}, A_u	7.66	0.0722	11.7	6.22	94.4	6.0[a]	6.60[c]
$1^3\Sigma_u^-$	π^*	A_u	8.63	0.1140	13.3	6.99	94.3	7.1[a]	7.38[c]
$1^3\Pi_u$	s	B_{2u}, B_{3u}	8.47	0.1781	21.1	8.19	95.6	8.06[d], 8.07[a,e]	8.25[f]
$1^3\Pi_g$	p_σ	B_{2g}, B_{3g}	8.53	0.2775	15.7	8.43	95.9	8.55[b],8.89[e], 8.90[a], 8.91[d]	8.74[f]
$1^3\Sigma_g^+$	p_π	A_g	8.86	0.8306	39.5	8.80	96.7	8.98[a], 9.06[e], 9.08[d]	9.07[g]
$1^3\Delta_g$	p_π	A_g, B_{1g}	8.94	0.8293	39.4	8.88	96.7	8.89[e], 8.91[d], 9.08[a]	9.16[g]
$1^3\Sigma_g^-$	p_π	B_{1g}	9.02	0.8796	40.9	8.96	96.7		9.24[g]
$2^3\Pi_u$	d_σ	B_{2u}, B_{3u}	9.67	0.5848	23.9	9.42	95.7	9.17[a,e], 9.18[d]	9.50[f]
$2^3\Sigma_u^+$	d_π	B_{1u}	9.94	0.9778	51.0	9.84	96.6		9.97[g]
$2^3\Delta_u$	d_π	B_{1u}, A_u	10.04	0.9327	49.5	9.83	96.4		10.01[g]
$2^3\Sigma_u^-$	d_π	A_u	10.18	0.8971	48.5	9.84	96.1		10.05[g]
$3^3\Pi_u$	d_δ	B_{2u}, B_{3u}	10.00	0.9712	65.7	9.91	96.0		10.01[f]
$1^3\Phi_u$	d_δ	B_{2u}, B_{3u}	10.00	0.9712	70.4	9.91	96.0		10.01[f]
$1^3\Sigma_u^+$	π^*	B_{1u}	5.56	0.0060	10.2	5.26	96.4	5.2[a]	5.61[c]
$1^3\Delta_u$	π^*	A_u, B_{1u}	6.75	0.0084	10.6	6.20	96.0	6.0[a]	6.60[c]
$1^3\Sigma_u^-$	π^*	A_u	7.39	0.0152	10.9	6.90	96.1	7.1[a]	7.38[c]
$2^3\Sigma_u^+$	d_π	B_{1u}	9.54	1.0017	52.0	9.82	97.2		9.97[g]

[a] From [1] [b] See text [c] From [18]
[d] From [50] [e] From [31] [f] From [22]
[g] From [23] [h] From [33]

vestigation of the level shift (See Table 3) also shows that the excitation energy increases with increasing reference weight. The calculation with the changed active space predicts an excitation energy of 10.65 eV and a fairly large TDM. The energy is higher than what we found for the *d* states of the first Rydberg series. Nevertheless, the value for $2^1\Sigma_u^+$ still has to be regarded as preliminary. An influence of higher Rydberg shells which are not included in our calculations cannot be ruled out. The predicted TDM is important in connection with an ongoing discussion about a third valence state in the VUV-spectrum of acetylene. The existance of such a state (labeled $\tilde{E}$ by Herzberg [2]) was first proposed by Wilkinson [51]. It is believed to generate intensity in the optical spectrum in the region 9.25–9.30 eV. Some groups, however, assign this structure to a bent valence state, either a planar *trans* bent state of C_{2h} symmetry [52] or a nonplanar near–*cis* state of C_2 symmetry [53]. The latter authors predict an *A* symmetry for the relevant state which, if true, would exclude the possiblity that this state is related to the $2^1\Sigma_u^+$ state of the linear molecule since Σ_u^+ correlates with IRREP B in C_2. Because of the ongoing discussion about high-lying states with bent structures [16], a careful investigation of excited states of *cis* and *trans* bent structures in the region of and above the first Rydberg series is highly desirable.

Before we turn to the lower lying valence states in nonlinear geometries, we briefly discuss the results for the Rydberg states. As mentioned in the Introduction, there are no recent calculations on Rydberg triplet states. This is astonishing given the fact that the energy difference between corresponding singlet and triplet Rydberg states provides additional information for the assignment of these states. The acetylene cation is linear [54] and there is little doubt that Rydberg states are linear, too. Vibrational progressions observed for some low-lying Rydberg states show mostly the C-C stretching mode with an energy of about 1800 cm^{-1}, similar to what is observed for the cation. The (0,0) transition is usually the most intense one, which means it is appropriate to compare the energy of the (0,0) transitions with calculated vertical excitation energies (Table 6).

The singlet Rydberg states of acetylene were recently reexamined by Peric et al. [54]. The assignments for the first series preferred by these authors are shown in Table 6 together with their and our theoretical results. There is very little doubt that an assignment of $1^1\Pi_g(p_\sigma)$ to the band at 9.01 eV, which was discussed at least as a possibility in several investigations [1, 32, 50], is not correct. $1^1\Pi_g(p_\sigma)$ should appear about half an eV below $1^1\Delta_g$ (p_π). The alternative assignment of this band to $1^1\Delta_g$ discussed in [1, 32, 50] and supported by experiments of Ashfold et al. [55] is much more likely on the basis of the present calculations.

The calculated differences between corresponding singlet and triplet Rydberg states are fairly small (Table 6). The largest splitting is predicted for $1\Sigma_g^+$ (p_π) and this band shows indeed the largest experimentally known energy difference among the first six Rydberg excitations, although the singlet to triplet shift is somewhat exaggerated in our calculation. The only open question about the assignment of the lower-lying triplet Rydberg states of the first series concerns $1^3\Pi_g$ and $1^3\Delta_g$. Wilden et al. [31] assigned a peak at 8.89 eV to either one of these two states. A peak at 8.55 eV, observed by the same authors under conditions where triplet states are enhanced, does not fit in a progression of the $1^3\Pi_u$ transition with a mean spacing of 1750 cm^{-1} and was therefore attributed to an additional vibrational level of $1^3\Pi_u$. Considering the otherwise very regular vibrational

structure of the two low-lying $1\Pi_u$ Rydberg transitions, an assignment of the peak at 8.55 eV to $1^3\Pi_g$ is proposed on the basis of the present calculations. A noticeable blueshift between singlet and triplet transitions is only predicted for $1\Sigma_g^-$ (p_π) and Σ_u^+ ($d\pi$), but no appropriate experimental information is available in these cases.

As far as the higher members of the first Rydberg series are concerned, we can only refer to the experimental results of Wilden et al. [31] and Allan [1], which show little differences between singlet and triplet enhanced spectra in this energy range (compare Fig. 2). This is in agreement with the very narrow shifts predicted for the upper four members of the first Rydberg series.

3.3 Geometries and energies of bent states

To derive theoretical estimates for the onset of vibrational progressions that may continue up to and even beyond the vertical excitation energy, we performed geometry optimizations at the CASSCF level for the lowest three excited singlet and the first four triplet states of *cis* and *trans* bent acetylene in C_{2v} and C_{2h} symmetry, respectively (Table 7). As these states lie vertically well below the onset of the first Rydberg series, and because of the fact that we did not find any indication of valence-Rydberg mixing for the corresponding vertically excited states, the optimization was performed with the *valence basis set* and the active space defined as *extended valence space* in Sect. 2.2. The geometry of the lowest excited singlet state and the two lowest triplet states was further optimized at the CASPT2 level using the *valence basis* and the *reduced valence space* in the procedure described in Sect. 2.2 (see Table 8).

A comparison of the bond lengths and bond angles (α) collected in Tables 7 and 8 shows no significant influence of the PT2 correction on the geometry. Only the C—H bonds are shortened by about 1.5 pm, but this may be due to the fact that the lowest occupied valence MO has been excluded from the active space during CASPT2 geometry optimization. The reliability of the CASSCF optimized geometries is further confirmed by a comparison with data from the literature. Table 7 shows results from what we consider the most elaborate calculations published until now. In spite of the fact that these data come from different sources, the lengthening of the central C—C bond (11 pm on average), and especially the changes in the bond angle α, show the same trends as our calculations. The absolute values of our bond lengths are, on average, 2 pm longer than the literature values. The only experimental geometry that is known for an excited state is the one for the *trans* bent 1^1A_u : $r_{CC} = 1.383$ Å/1.388 Å, $r_{CH} = 1.07-1.09$ Å, and $\alpha = 120.2°$ [5, 6]. These values compare extremely well with our theoretical results. The C—C bond length seems to show that our, compared to the literature, slightly longer bond lengths are correct. The experimental C—H bond length, on the other hand, indicates that the shortening of this bond predicted by the PT2 correction tends in the right direction.

As far as energies are concerned, we have few reliable experimental data which can be used for a comparison. The adiabatic transition to 1^1A_u has been observed at 5.23 eV [5, 6]. If this is really the (0,0) transition of the experimentally observed band, it agrees extremely well with the 5.14 eV obtained for the CASPT2 optimized geometry and the 5.19 eV found for the CASSCF optimized geometry. The result of what we consider the most elaborate calculation to be found in the literature is 5.39 eV [10].

Wendt et al. [56] observed a transient absorption at 0.92 eV which they assigned to a transition from the lowest triplet state on the *cis* side (1^3B_2) to the second *cis* triplet state (1^3A_2). Our calculations predict 0.96 eV, in close agreement with the 0.94 eV obtained by Yamaguchi et al. [14]. The combined information from the theoretical investigations [10] narrows the margin for the location of the first triplet state 1^3B_2, which is not known experimentally, to 3.75 ± 0.15 eV. The last piece of experimental information that is useful in the present context is a band observed in the UV absorption spectrum by Foo and Innes [7]. The band starts at 6.71 eV and shows a well-resolved vibrational structure which will be discussed in more detail in the next section. Foo and Innes assigned the band to a transition from the linear ground state to the second excited singlet state 1^1B_u on the *trans* side. This assignment agrees with the result of our CASPT2 calculations, which yield 6.68 eV for this transition (Table 7). It has to be mentioned, however, that recent EOM-CCSD calculations [9, 10] predict structures of reduced symmetry for S_2 and T_3 on the *cis* as well as on the *trans* side. The minima found for

Table 6. Comparison of theoretical and experimental energies for the singlet and triplet states of the first Rydberg series

State	Char.	Exp.	Singlet			Triplet			Δ_{T-S}
			Peric[a]	This work	Exp.	Demoulin[b]	This work	Exp.	This work
$1\Pi_u$	s	8.16[c]	8.0	8.30	8.07[g]	8.25	8.19	−0.09	−0.11
$1\Pi_g$	p_σ		8.4	8.60	8.55[h]	8.74	8.43		−0.17
$1\Sigma_g^-$	p_π		8.9	8.92		9.24	8.96		0.04
$1\Delta_g$	p_π	9.02[d]	8.9	8.96	8.89[g]	9.16	8.88	−0.13	−0.08
Σ_g^+	p_π	9.21[d]	9.0	9.06	9.06[g]	9.07	8.80	−0.15	−0.26
$2\Pi_u$	d_σ	9.24[c]	9.4	9.55	9.17[g]	9.50	9.42	−0.07	−0.13
Σ_u^+	d_π	9.27[c]	9.4	9.65		9.97	9.84		0.19
$2\Sigma_u^-$	d_π		9.8	9.81		10.05	9.84		0.03
$2\Delta_u$	d_π	10.00[e]	9.8	9.85		10.01	9.83		−0.02
$1\Phi_u$	d_δ	9.91[f]	9.8	9.93		10.01	9.91		−0.02
$3\Pi_u$	d_δ	9.98[c]	9.8	9.93		10.01	9.91		−0.02

[a] From [20, 54]
[b] From [22, 23]
[c] From [49]
[d] From [55]
[e] From [61]
[f] From [62]
[g] From [31]
[h] See text

these states with the symmetry restricted to either C_{2v} or C_{2h} were connected with one imaginary frequency on the *trans* side and two such frequencies on the *cis* side. A C_s minimum was found for S_2 on the *cis* side, which is about 0.7 eV lower in energy than the C_{2v} structure. If S_2 is really highly asymmetric and strongly stabilized with respect to the *cis* (and the *trans*) form, the whole vibrational structure starting at 6.71 eV has to be interpreted completely different from what was proposed until now, e.g. as a transition to the Frank-Condon region with the onset of the corresponding band strongly suppressed because of the large geometry change between initial and final state. However, this does not explain the absence of any reasonable intensity below 6.71 eV in the optical spectra [3] and in EEL spectra that were measured under optical conditions [32]. Up to now the spectroscopic evidence is in favor of a transition that starts at 6.71 eV.

3.4 Geometries and energies of linear states

It is known that the linear geometries of the low-lying valence states are higher-order saddlepoints and not transition states for the isomerization between *cis* and *trans* bent structures [11, 14]. However, the location of these linear states indicates the region in which a vibrational progression that departs from the adiabatic transition to a related state of a bent structure should exhibit the strongest deviation from a regular pattern. To find out how far below the vertical excitations discussed in Sect. 3.2 these regions are to be expected, we calculated optimized bond lengths and corresponding energies for the linear geometry of the first two excited singlet states and for the first two triplet states. As these states are well separared from the onset of the first Rydberg series, the calculations also could be done with the *valence basis* and the *extended valence space*. The results are shown in Table 9.

Table 7. Geometries of the bent states obtained from a CASSCF optimization and corresponding CASPT2 energies. Geometries and energies shown in the second line for each state are values from calculations found in literature

			CASSCF				CASPT2		Exp.
			r_{CC} (Å)	r_{CH} (Å)	α	ΔE (eV)	ΔE (eV)	Ref. (%)	ΔE (eV)
cis	S_1	1^1A_2	1.355	1.111	132.0	5.89	5.59	95.2	
			1.325[a]	1.093	134.4		5.85[h]		
	S_2	1^1B_2	1.346	1.127	135.8	7.12	6.60	94.7	
			1.329[c]	1.090	145.2		6.93[h]		
	S_3	2^1A_2	1.328	1.080	169.7	7.50	6.82	94.3	
			1.323[c]	1.065	172.4		7.27[c]		
	T_1	1^3B_2	1.346	1.102	128.3	3.81	3.74	95.6	
			1.327[d]	1.083	128.2		3.82[d]		
	T_2	1^3A_2	1.374	1.104	129.9	4.84	4.70	95.5	
			1.340[b]	1.089	132.5		4.76[d]		
	T_3	2^3B_2	1.346	1.081	163.1	6.08	5.57	94.5	
			1.336[c]	1.067	166.0		5.78[h]		
	T_4	2^3A_2	1.347	1.084	163.7	6.78	6.31	94.6	
			1.334[c]	1.068	167.9		6.72[c]		
trans	S_1	1^1A_u	1.389	1.109	120.0	5.40	5.19	95.5	5.23[e]
			1.358[a]	1.091	123.6		5.39[h]		
	S_2	1^1B_u	1.350	1.092	146.1	7.35	6.68	94.2	6.65[f], 6.71[g]
			1.336[c]	1.081	146.0		7.03[h]		
	S_3	2^1A_u	1.325	1.078	168.1	7.49	6.83	94.3	
			1.323[c]	1.065	171.4		7.27[c]		
	T_1	1^3B_u	1.350	1.093	130.0	3.94	4.04	96.7	< 4.367[f]
			1.329[d]	1.076	131.4		4.16[d]		
	T_2	1^3A_u	1.398	1.106	119.1	4.47	4.41	89.2	
			1.368[b]	1.088	122.3		4.44[d]		
	T_3	2^3B_u	1.368	1.081	146.8	5.93	5.46	92.5	
			1.338[h]	1.061	154.9		5.69[h]		
	T_4	2^3A_u	1.345	1.080	157.3	6.76	6.28	92.9	
			1.336[c]	1.067	164.1		6.72[c]		

[a] From [13] [b] From [12]
[c] From [18] [d] From [14]
[e] From [5,6] [f] From [8] [g] From [7] [h] From [9,10]

Table 8. Geometries and energies for planar *cis* and *trans* bent structures obtained from a CASPT2 geometry optimzation

			CASSCF				CASPT2	
			r_{CC} (Å)	r_{CH} (Å)	α (°)	ΔE (eV)	ΔE (eV)	Ref. (%)
	S_0	1^1A_g	1.217	1.066	180	–	–	96.2%
cis	S_1	1^1A_2	1.353	1.097	132	5.90	5.55	95.2%
	T_1	1^3B_2	1.349	1.088	128	3.81	3.69	95.6%
	T_2	1^3A_2	1.368	1.090	130	4.84	4.66	95.5%
trans	S_1	1^1A_u	1.382	1.094	122	5.40	5.14	95.3%
	T_1	1^3B_u	1.359	1.078	133	3.95	3.98	94.5%
	T_2	1^3A_u	1.392	1.091	121	4.47	4.32	95.8%

Again the PT2 correction has little influence on the optimized geometry. Only for $S_1(1^1\Sigma_u^-)$ did we observe a slightly increased C—C bond length (1.2 pm) at the CASPT2 level. The energies for the adiabatic transitions at linear geometry are between 0.43 eV and 0.97 eV lower than for the vertical excitations. The largest stabilization due to relaxation of the bond lengths is found for S_1. The energy difference between the relaxed linear S_1 state and the *cis* and *trans* bent states is reduced to 0.44 eV and 0.85 eV, respectively. Bands that result from a transition from the linear ground state to 1^1A_u (S_1 of the *trans* bent structure) or 1^1A_2 (S_1 of the *cis* bent structure) are therefore expected to exhibit pronounced anharmonicities and low intensities in the vicinity of the (0,0) transitions because of unfavorable Frank-Condon factors. For the optical allowed transition to 1^1A_u, this is well known. The band shows a complicated vibrational fine structure which starts with a spacing of $1047\,cm^{-1}$ [57]. Up to level 6 the vibronic bands form a progression with an anharmonicity constant of about $10\,cm^{-1}$. Between level 6 at 5.97 eV [58] and level 7 at 6.08 eV [59] the spacing drops suddenly by nearly $100\,cm^{-1}$. This is just the energy where we find the linear barrier in our calculations. For S_2 the situation is more complicated. Starting at 6.71 eV the optical spectrum shows a series of well-resolved vibronic bands. The spacings between the first six members of this series are 734, 688, 747, 699, and $843\,cm^{-1}$. Foo and Innes [7] assigned the band at 6.71 eV to the onset of an optically allowed transition to S_2 (1^1B_u) on the *trans* bent side. If this assignment is correct, the observed irregularities in the vibrational spacings can be attributed to the fact that the S_2 minimum on the *trans* side is predicted to lie only 0.19 eV ($1530\,cm^{-1}$) below the linear barrier. If, however, the real S_2 minima corresponds to the C_s structure discussed in the last section, it is necessary to assign these vibronic bands to higher vibrational levels of S_2.

3.5 The EEL spectrum in the energy range below 7 eV

Gas-phase EEL spectra measured under conditions which enhance transitions to triplet states (low impact energy and large scattering angle) show a broad band with partially resolved vibrational fine structure that starts around 4.4 eV and extends beyond 8 eV [32]. All the intensity observed below 6 eV was assigned to a single triplet state, presumably 1^3A_u, the second triplet state on the *trans* side. A possible contribution of S_1 to this energy range can be ruled out by comparison with spectra measured under optical conditions (high impact energy and small scattering angle) [32]. Recent high-resolution EEL investigations of solid-phase acetylene [8] raised some questions about this interpretation. The vibrational fine structure observed between 4.4 eV and 5.6 eV does not fit into a single progression. Instead, it consists of three different parts: an irregular section between 4.43 eV and 4.56 eV, a short progression with three members and a spacing of $800\,cm^{-1}$ between 4.62 eV and 4.82 eV, and a longer progression with an average spacing of $680\,cm^{-1}$ between 4.97 eV and 5.56 eV. The latter was assigned to 1^3A_u in spite of the fact that a total symmetric vibration of $680\,cm^{-1}$ did not agree with theoretical predictions for the normal modes of this state [12, 14].

Based on the present theoretical results we attempt a reinterpretation of the EEL spectrum of acetylene up to an energy of about 8 eV. The experimental spectrum is shown in Fig. 4. Spectroscopic details which are hardly visible in this survey spectrum can be found elsewhere [8]. The spectrum was measured under conditions which enhance transitions to triplet states. The overall agreement with gas-phase EEL spectra measured under similar conditions [32] assures that transitions to singlet states do not contribute to the observed intensity below 6.6 eV. The theoretical results are indicated as bars that stretch from the adiabatic transitions for the planar *trans* and *cis* bent structures to the vertical transitions. Below the linear barrier between *cis* and *trans* bent structures (see Sect. 3.4) these bars are shaded in a different way.

Without a theoretical guideline it is difficult to understand the break in the vibrational structure at 4.6 eV and the irregular pattern observed between 4.34 eV and 4.56 eV. It is now quite obvious that the irregularities below 4.6 eV are connected with the linear barrier in T_1 for which we calculate 4.62 eV. The assignment of the two progressions (4.62–4.82 eV and 4.97–5.6 eV) is more difficult. The average spacing between the eight members of the higher energy one is 84.3 meV ($680\,cm^{-1}$). Corresponding structures have been observed in gas-phase EEL spectra [32]. The progression is anharmonic with an approximate anharmonicity constant of $10\,cm^{-1}$. The anharmonicity is similar to what was found for the first members of the progression observed in the optically detected transition to $S_1(1^1A_u)$ on the *trans* bent side but the vibrational energy is considerably lower (compare Sect. 3.4). Extrapolation of the progression to the onset of 1^3A_2 at 4.66 eV and 1^3A_u at 4.32 eV leads to vibrations of approximately $800\,cm^{-1}$ and $880\,cm^{-1}$, respectively. The former value compares well with the

Table 9. Geometries and energies of linear barriers on the potential energy surfaces of excited singlet and triplet states

		CASSCF			CASPT2			Lit.	ΔE_{vert} (eV)
		r_{CC} (Å)	r_{CH} (Å)	ΔE (eV)	r_{CC} (Å)	r_{CH} (Å)	ΔE (eV)		
S_1	$1^1\Sigma_u^-$	1.329	1.074	7.21	1.341	1.067	5.99		6.96
$S_{2/3}$	$1^1\Delta_u$	1.320	1.076	7.51	1.322	1.061	6.87		7.30
T_1	$1^3\Sigma_u^+$	1.357	1.076	4.87	1.356	1.067	4.63	4.61[a]	5.26
$T_{2/3}$	$1^3\Delta_u$	1.341	1.074	6.19	1.347	1.067	5.64	5.74[a]	6.20

[a] From [11]

$771\,cm^{-1}$ that has been observed at the onset of the transient absorption assigned to $1^3B_2 - 1^3A_2$. A theoretical value for the harmonic frequency of the bending mode of $836\,cm^{-1}$ was determined in [12]. The resulting scaling factor of 0.922 appears quite normal.

An assignment of the long progression to 1^3A_u as proposed [8] becomes unlikely in the light of the present analysis. The unscaled harmonic frequency calculated for 1^3A_u is $1137\,cm^{-1}$ [12]. With the above-mentioned scaling factor this leads to an estimate of $1050\,cm^{-1}$. Even with the uncertainties embedded in the scaling procedure and in the extrapolation of the progression, the difference of $170\,cm^{-1}$ is much too large to connect the observed progression with 1^3A_u. It is also very unlikely that the calculation is so far off in this case. The calculated value for the bending vibration of 1^1A_u is $1107\,cm^{-1}$ [13] and this value compares well with the experimentally observed $1049\,cm^{-1}$ [5] if scaled by 0.922. A further arguement in favor of an assignment of the long progression to 1^3A_2, the second triplet state on the *cis* side, is the fact that the progression ends just where it approaches the calculated linear barrier of T_2. A comparison with the irregularities observed in the optical S_1 spectrum in the vicinity of the linear barrier suggests that the vibronic pattern of T_2 should become even more complicated (and therefore no longer resolvable with the given resolution) at this point because of the additional influence of the Renner-Teller effect.

An alternative to an assignment of the long progression to 1^3A_2 is an assignment to either T_1 or T_3. If T_3 is nonplanar, as found by Cui et al. [10], our calculated adiabatic excitation energies are only upper bounds for the real values, which may be several tenths of an eV lower [10]. However, a strongly nonplanar structure should lead to small Franck-Condon factors. It is therefore unlikely that a progression which is clearly visible down to 5 eV results from a nonplanar T_3. On the other hand, this state is certainly responsible for some of the increased intensity that is observed above 5.7 eV. The other alternative, T_1, is not easily discarded. The center of the progression coincides with what we calculate for the vertical T_1 transition and lies well above the linear barrier. In this region the bending vibrations should be fairly regular. Since model calculations for the intensity distribution close to a lower-symmetry minimum or in the range above the linear barrier do not exist, it is hard to opt for one of the alternative assignments. Furthermore, the intensity distribution in EEL spectra is more difficult to predict than in the case of optical spectra.

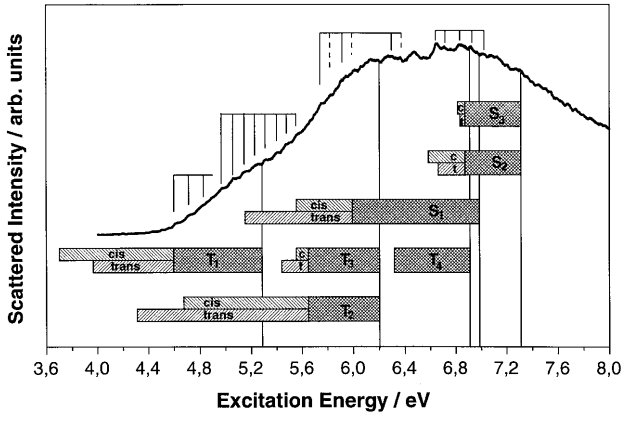

Fig. 4. Solid-state low-energy EEL spectrum of acetylene [8]. Indicated are the spectral regions as assigned in this work (see text for details)

It is tempting to assign the short progression between 4.62 eV and 4.82 eV also to 1^3A_2 because of the close coincidence of the $800\,cm^{-1}$ spacing with the $771\,cm^{-1}$ observed in the transient $1^3B_2 - 1^3A_2$ absorption. However, this assignment faces two problems:

1. Because of the incompatibility of the two progressions it requires an assignment of the long progression to T_1.
2. Franck-Condon unfavorable transitions to the onset of the 1^3A_2 band become visible instead of the higher members of this progression, which are expected to have the larger FC factors. Therefore it is more likely that the short progression belongs to the T_1 system and is located slightly above the linear barrier.

We now turn to the spectral range between 5.6 eV and 7 eV (Fig. 4). The vibronic bands observed at 6.65, 6.73, 6.83, 6.92, and 7.03 eV correspond to the bands in the optical spectrum that were assigned to 1^1B_u, the second singlet state on the *trans* bent side (see Sect. 3.3). It is interesting to note that this vibronic structure is not as pronounced in the triplet enhanced EEL spectrum as in the optical spectra. The absence of any noticeable intensity below 6.6 eV in the EEL spectra under optical conditions ensures that the intensity observed between 5.6 eV and 6.6 eV in Fig. 4, and in other EEL spectra that were measured under conditions that enhance transitions to triplet states, results from triplet states only. The vibronic bands at 5.76, 5.83, 5.93, 6.01, 6.28, and 6.36 eV fit into the progressions $(5.76 + n \times 0.174)$ eV and $(5.76 + 0.100 + n \times 0.174)$ eV with $n = 1, 3$. As these bands lie above the linear barrier of $1^3\Delta_u$ ($T_{2,3}$), we assign them to a direct transition to $1^3\Delta_u$. This transition shows the progression of a mode of about $1400\,cm^{-1}$ that might be the $1\sigma_g^+$ (symmetric CC stretch mode) of the linear molecule and a repetition of this progression with a false origin of $800\,cm^{-1}$, probably corresponding to the bending mode of the system.

The structure at 6.47 eV was tentatively assigned to $T_4(1^3\Sigma_u^-)$ [8]. With the new theoretical results at hand, this assignment becomes highly probable. Also, with a vertical excitation energy of 6.99 eV this state extends well into the region of the S_2 transition. This could explain why the vibronic structure in this region is less pronounced in the triplet-enhanced EEL spectra than in the optical ones. Additional preliminary results for T_4 indicate that this state may not be planar and that its minimum lies three or four tenths of an eV below the 6.3 eV calculated for the planar structures, which are very close to linearity. It is therefore likely that T_4 contributes to the intensity between 6 eV and 6.3 eV and obscures part of the progressions assigned to $1^3\Delta_u$.

4 Conclusion and outlook

The analysis of the EEL spectra of acetylene on the basis of CASPT2 leads to some reassignments in relation to the low-lying triplet states. Some of these assignments are still tentative and further theoretical and experimental work is necessary to clarify the open questions.

The work presented is the first step in an attempt to describe the triplet states of acetylene and the corresponding spectra by means of time independent and time dependent ab initio quantum chemistry. The next step will be the calculation of PES for the three lowest triplet states that are believed to determine the shape of the spectrum in the low-energy region. After that, a quantum dynamical approach using wave packet dynamics on the Renner-Teller coupled potential energy surfaces is planned.

Acknowledgements. The authors would like to thank Prof. Dr. B.O. Roos, Dr. M.P. Fülscher (Lund University, Sweden) and Dr. H. Köppel (University of Heidelberg) for fruitful discussions and Prof. Dr. S. Peyerimhoff and Dr. M. Peric (Universities of Bonn and Belgrade) for providing their reexamination of the singlet Rydberg states prior to publication. Part of the calculations was performed at the Regionale Rechenzentrum der Universität zu Köln. The research was supported by the Schwerpunktprogramm "Zeitabhängige Phänomene und Methoden in Quantensystemen in der Physik und Chemie" of the Deutsche Forschungsgemeinschaft. Financial support of the Fonds der Chemischen Industrie is also acknowledged.

References

1. Dressler R, Allan M (1987) J Chem Phys 87:4510
2. Herzberg G (1966) Electronic spectra of polyatomic molecules. Van Nostrand Reinhold, New York
3. Robin MB (1975) Higher excited states of polyatomic molecules, vol 2. Academic, New York
4. Nakayama T, Watanabe K (1964) J Chem Phys 40:558
5. Ingold CK, King GW (1953) J Chem Soc 2702, 2704, 2708, 2725, 2745
6. Innes KK (1954) J Chem Phys 22:863
7. Foo PD, Innes KK (1973) Chem Phys Lett 22:439
8. Swiderek P, Michaud M, Sanche L (1997) J Chem Phys 106:9403
9. Cui Q, Morokuma K (1997) Chem Phys Lett 272:319
10. Cui Q, Morokuma K, Stanton JF (1996) Chem Phys Lett 263:46
11. Vacek G, Sherrill D, Yamaguchi Y, Schaefer HF III (1996) J Chem Phys 104:1774
12. Sherrill D, Vacek G, Yamaguchi Y, Schaefer HF III, Stanton JF, Gauss J (1996) J Chem Phys 104:8507
13. Stanton JF, Huang C-M, Szalay PG (1994) J Chem Phys 101:356
14. Yamaguchi Y, Vacek G, Schaefer HF III (1993) Theor Chim Acta 86:97
15. Vacek G, Thomas JR, DeLeeuw BJ, Yamaguchi Y, Schaefer HF III (1993) J Chem Phys 98:4766
16. Lievin J (1992) J Mol Spectrosc 156:123
17. Peric M, Peyerimhoff SD, Buenker RJ (1987) Mol Phys 62:1339
18. Lischka H, Karpfen A (1986) Chem Phys 102:77
19. Peric M, Peyerimhoff SD, Buenker RJ (1985) Mol Phys 55:1129
20. Peric M, Buenker RJ, Peyerimhoff SD (1984) Mol Phys 53:1177
21. Wetmore RW, Schaefer HF III (1978) J Chem Phys 169:1648
22. Demoulin D (1975) Chem Phys 11:329
23. Demoulin D, Jungen M (1974) Theor Chim Acta 34:1
24. Kammer WE (1970) Chem Phys Lett 6:529
25. Lundberg JK, Chen Y, Pique J-P, Field RW (1992) J Mol Spectrosc 156:104
26. Dupré P, Green PG, Field RW (1995) Chem Phys 196:211
27. Dupré P, Jost R, Lombardi M, Green PG, Abramson E, Field RW (1991) Chem Phys 152:293
28. Humphrey SJ, Morgan CG, Wodtke AM, Cunningham KL, Drucker S, Field RW (1997) J Chem Phys 107:49
29. Drucker S, O'Brien JP, Patel P, Field RW (1997) J Chem Phys 106:3423
30. Hammond P, Jureta J, Cvejanovic D, King GC, Read FH (1987) J Phys B 20:3547
31. Wilden DG, Comer J, Taylor S (1980) J Phys B 13:2849
32. Wilden DG, Hicks PJ, Comer J (1977) J Phys B 10:L403
33. Robin MB (1985) Higher excited states of polyatomic molecules, vol 3. Academic, New York
34. Petelin AN, Kiselev AA (1972) Int J Quant Chem 6:701
35. Malmqvist PA, Rendell A, Roos BO (1990) J Phys Chem 94:5477
36. Roos BO, Fülscher MP, Malmquist P-A, Merchan M, Serrano-Andres L (1995) In: Langhoff SR (ed) Quantum mechanical electronic structure calculations with chemical accuracy. (Understanding Chemical Reactivity, vol 13) Kluwer Dordrecht, p 357
37. Roos BO, Andersson K (1995) In: Yarkony DR (ed) Modern electronic structure theory, part I. (Advanced Series in Physical Chemistry, vol 2), World Scientific, Singapore, p 55
38. Roos BO, Andersson K, Fülscher MP, Malmqvist P-A, Serrano-Andres L, Pierloot K, Merchan M (1996) Adv Chem Phys 93:219
39. Almlöf J, Taylor PR (1991) Adv Quantum Chem 22:301
40. Widmark P-O, Persson BJ, Roos BO (1990) Theor Chim Acta 77:291
41. Andersson K, Malmqvist PA, Roos BO, Sadlej AJ, Wollinski K (1990) J Phys Chem 94:5483
42. Andersson K, Malmqvist PA, Roos BO (1992) J Chem Phys 96:1218
43. Roos BO, Andersson K (1995) Chem Phys Lett 245:215
44. Roos BO, Andersson K, Fülscher MP, Serrano-Andres L, Pierloot K, Merchan M, Molina V (1996) J Mol Struct 388:257
45. Andersson K, Blomberg MRA, Fülscher MP, Karlström G, Kellö V, Lindh R, Malmqvist P-A, Noga J, Olsen J, Roos BO, Sadlej AJ, Siegbahn PEM, Urban M, Widmark P-O (1994) *MOLCAS* version 3
46. Baldacci A, Ghersetti S, Hurlock SC, Rao KN (1976) J Mol Spectrosc 59:116
47. Malmqvist PA (1986) Int J Quantum Chem 30:479
48. Malmqvist PA, Roos BO (1989) Chem Phys Lett 155:189
49. Herman M, Colin R (1982) Phys Scr 25:275
50. Hammond P, Jureta J, Cvejanovic D, King GC, Read FH (1987) J Phys B 20:3547
51. Wilkinson PG (1958) J Mol Spectrosc 2:387
52. Herman M, Colin R (1981) J Mol Spectrosc 85:449
53. Lundberg JK, Jonas DM, Rajaram B, Chen Y, Field RW (1992) J Chem Phys 97:7180
54. Peric M, Peyerimhoff SD (1998) In: Sandorfy C (ed) The role of Rydberg states in spectroscopy and reactivity. Kluwer, Dordrecht (in press)
55. Ashfold MNR, Tutcher B, Yang B, Jin ZK, Anderson SL (1987) J Chem Phys 87:5105
56. Wendt HR, Hippler H, Hunziker HE (1979) J Chem Phys 70:4044
57. Watson JKG, Herman M, van Craen JC, Colin R (1982) J Mol Spectrosc 95:101
58. van Craen JC, Herman M, Colin R, Watson JKG (1985) J Mol Spectrosc 111:185
59. van Craen JC, Herman M, Colin R, Watson JKG (1986) J Mol Spectrosc 119:137
60. Zhu YF, Shehadeh R, Grant ER (1993) J Chem Phys 99:5723
61. Fillion JH, Campos A, Pedersen J, Shafizadeh N, Gauyacq D (1996) J Chem Phys 105:22
62. Ashfold MNR, Dixon NR, Prince JD, Tutcher B, (1985) Mol Phys 56:1185